J Indian Soc Remote Sens
DOI 10.1007/s12524-015-0470-4

RESEARCH ARTICLE

ISRS

Integrated Remote Sensing and Structural Analysis Studies of Tayyib Al-Ism Area, Northwestern Arabian Shield, Saudi Arabia

Osama M. K. Kassem[1,2] · Habes A. Ghrefat[1] · Haider Zaman[3] · Awni T. Batayneh[4] · Saad Almogren[1] · Yousef Nazzal[5] · Eslam Elawadi[6]

Received: 11 February 2014 / Accepted: 19 June 2015

Abstract Geological and structural mappings of Tayyib Al-Ism area were carried out using the rocks finite strain data, the Landsat-7 Enhanced Thematic Mapper Plus (ETM+) data and the field based observations. To analyze the finite strain in the studied rocks, the R_f/ϕ and Fry methods are applied to feldspar porphyroclasts and mafic grains from nine metavolcano-sedimentary samples (Hegaf Formation), four diorite-gabbros suite samples (Sawawin Complex), two meta-granite samples (Ifal suite) and five Zuhd alkali granite samples. The obtained data indicate traces of high to moderate level of deformation in the meta-granite and metavolcano-sedimentary rocks. The axial ratios along the XZ section range from 1.70 to 4.80 for the R_f/ϕ method and from 1.50 to 4.50 for the Fry method. A sub-vertical trend of short axes in association with sub-horizontal foliation is also observed. These informations allow us to conclude that a finite strain in the deformed granitic rocks is of the same order of magnitude as in the metavolcano-sedimentary rocks. The contacts between the metavolcano-sedimentary and granitic rocks in Tayyib al Ism area were formed during the granitic intrusions along some of the faults under brittle to semi-ductile deformation conditions. These faults have significantly influenced the geometry and style of rifting in the Red Sea during the Neogene. The finite strain was accumulated in the area during the process of deformation, which superimpose the already existed nappe structure. It indicates that the nappe contacts formed during the accumulation of finite strain. In addition to finite strain analysis, band ratio images (3/1, 5/3, 7/5) and Principal Component Analysis (PCA) technique have been used, which proved effective in mapping geological and structural features of various rock bodies exposed in the study area.

Keywords Finite strain · Remote sensing · Tayyib al Ism · Arabian shield · Saudi Arabia

Introduction

The Arabia shield is divided into a number of allochthonous terranes separated by ophiolite-decorated sutures (Johnson 1998). Amalgamation of these terranes took place sometime between 600 and 680 Ma (Nehlig et al. 2002) as a result of collision between the East and West Gondwanaland, which consumed the intervening Mozambique Ocean. Many authors believe that the tectono-stratigraphic terranes in the Arabian shield are small to large crustal blocks bounded by major shear zones. As shown in Fig. 1, some of these sutures were formed as a result of oceanic lithosphere consumption by subduction and magmatic-arc convergence, while others are transcurrent faults representing the original sutures but predominantly zones of Late Neoproterozoic strike-slip motion (Johnson 1998). The well-documented sutures in the Arabian Shield include the Bi'r Umq suture between the Jeddah and Hijaz

✉ Osama M. K. Kassem
kassemo1@yahoo.com

1 SGSRC, Department of Geology, Faulty of Science, King Saud University, P.O. Box 2455, Riyadh 11451, Kingdom of Saudi Arabia

2 Department of Geology, National Research Center, Al-Behoos str., 12622 Dokki, Cairo, Egypt

3 Department of Geology, Faculty of Science, Taibah University, Madinah 41477, Saudi Arabia

4 Department of Earth and environmental Sciences, Yarmouk University, Irbid, Jordan

5 College of Art and Sciences, Applied Math and Sciences, Abu Dhabi University, Abu Dhabi, United Arab Emirates

6 Airborne Exploration Department, Exploration Division, Nuclear Materials Authority, Maadi, Cairo, Egypt

Published online: 31 July 2015

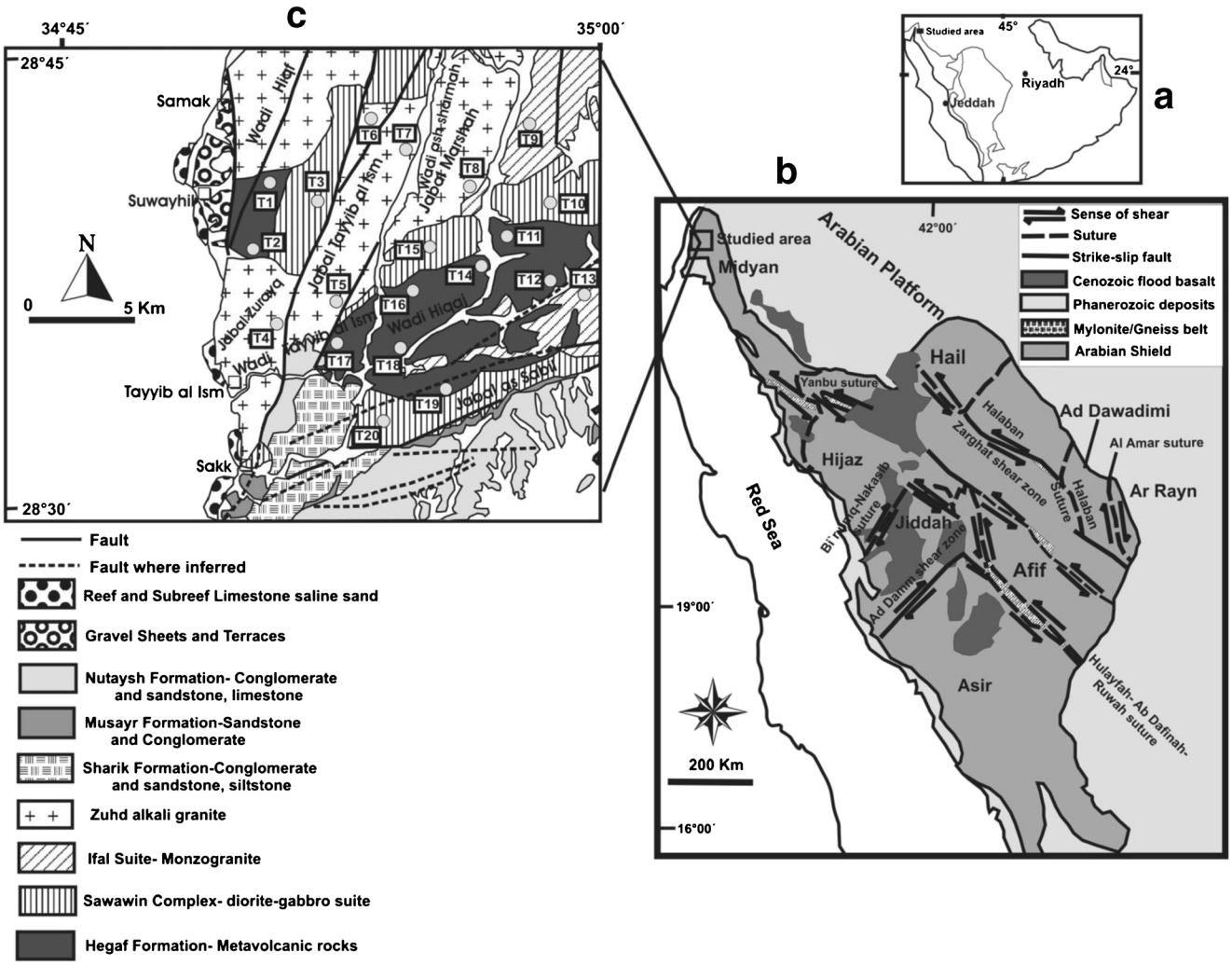

Fig. 1 **a** Location of the study area within the framework of Arabian Plate (inset). **b** Geological map of the Arabian Shield (modified from Stoeser and Camp 1985). **c** Generalized Geological map of Tayyib al Ism area showing sampling locations (modified from Clark 1986)

terranes (Johnson et al. 2003), a suture between the Afif and Hijaz-Jiddah-Asir terranes (Johnson and Kattan 2001); and the Yanbu suture between the Hijaz and Midyan terranes (Stoeser and Camp 1985). The Neoproterozoic Ad Damm Fault (strike-slip) separates the Asir Terrane from Jeddah Terrane, and the Al Amar Fault makes a boundary between the Ad Dawadimi and Ar Rayn terranes (Fig. 1b). Most of these terranes are the composite blocks of smaller sub-terranes. At present, these terranes are separated by major, mainly N-S and NE-SW, suture zones lined by serpentinized ultramafic rocks (ophiolites and tectonic slices) and by major NW-SE faults. Other than some gneissic structures, the entire Arabian Shield is only slightly metamorphosed, which constitutes one of the best preserved exposures of the Neoproterozoic assemblages. These assemblages were formed due to accretion of several volcanic-arcs, which are overlain to the east, north and south by a thick sedimentary cover of the Phanerozoic age.

The extent of the Neoproterozoic basement rocks has been traced in the Maqna area, northeast of the Midyan basin. This basement, which was formed along an accreting volcanic arc, is believed to be granitic in nature (Gardner et al. 1996). The basement rocks in the Midyan region consist of ultramafic, metavolcanic, metasedimentary and granitic rocks. The Tayyib al Ism area is located in the Midyan Peninsula that geologically makes a triangle shape structure between the Gulf of Aqaba and the Red Sea. This area is undergoing through tectonic activities as a result of continues blocks movements, which sometime produces seismic activities in the area. This study is thus undertaken to investigate the structural architecture of Tayyib Al-Ism area by finite strain analysis and remote sensing tools, which can shed light on its kinematic history. The main goal of applying remote sensing techniques is to identify and map various lithological units exposed in the Midyan Basin using Landsat 7 ETM+ data.

Spectral characteristics obtained from different remote sensing techniques are used here to map different geological, lithological and structural units in the study area. On the other hand, the aim of using structural analysis is to determine the mechanical behavior of faults and tectonic contacts, so that the nature and distribution of finite strain in the area could be documented.

Geological Description of the Study Area

The study area, named as Midyan region, is located in the northwestern part of the Arabian shield, northwestern Saudi Arabia. The area is bounded by the Gulf of Aqaba in the northeast and the Red Sea in the southwest. The rock bodies in the area are made of Proterozoic stratiform and intrusive rocks, the Paleozoic sandstones (in the east) and the Mesozoic-Cenozoic sedimentary successions (in the southwest). The rock units that cover the area consist of the Hegaf Formation, the Sawawin Complex, the Ifal suite, the Zuhd alkali granite, the Sharik Formation, the Musayr Formation, and the Nutaysh Formation (Fig. 1c).

The Hegaf Formation, which belongs to the Proterozoic stratiform rocks, is the oldest rock unit in the study area (Fig. 1c). This formation is composed of a variety of highly folded volcanic, volcaniclastic and subordinate epiclastic rocks, which are affected by greenschist facies metamorphism in general and up to hornfels grade in some areas. The metavolcanic rocks of the area are mainly andesitic in composition (Clark 1986), including the metamorphosed mafic and felsic tuffs, meta-andesite, metabasalt, amphibolites, hornfels, mica schist and metamorphosed siltstone (Davies and Grainger 1985).

The Sawawin Complex in the area is a heterogeneous mixture of metadiorites (granodiorite to gabbro) that intruded the Hegaf Formation (Fig. 1c). The diorite and quartz diorite bodies associated with tonalite and trondhjemite to the north of Wadi ash Sharmah are assigned to Sawawin Complex. Medium grained diorite and fine to medium grained quartz diorite, in which amphibole and biotite are partly altered to chlorite, are the most common rock types. Many of these mafic bodies are later intruded by granitic rocks of the Ifal suite as well as by numerous younger mafic dikes.

The Ifal Suite in the area is characterize by large, irregular shaped plutons of monzogranitic and granodioritic compositions that generally form the low relief areas traversed by numerous mafic, and felsic dikes (Fig. 1c). The monzogranites are coarse to very coarse grained in size and highly porphyritic. Because of its relatively younger age, the plutons of Ifal Suite intruded both the Sawawin complex and the Hegaf Formation. The Zuhd alkali granite is characterized by predominantly equigranular and coarse grained plutons, which reach up to 17 km in diameter at Jabal az Zuhd, Jabal Marshah and Jabal Tayyib al Ism (Fig. 1c). This group of granites is dissected by a series of faulted blocks from the Gulf of Aqaba fault system, which to great extent destroyed the original form of intrusions. The Zuhd granite in Jabal Tayyib al Ism consists of alkali quartz synite and porphyritic alkali microgranite.

The Mesozoic-Cenozoic sedimentary rocks in the study area generally overly the Proterozoic basement rocks with clear nonconformity, sedimentation and tectonism. The facies distribution and their lateral changes are the result of syn-sedimentation tectonic movements that affected the area in successive pulses since the Late Cretaceous. The faults with normal and sinistral movements were repeatedly reactivated, forming the sedimentary basins and basement highs. The Sharik Formation is mainly composed of red tinted thick units of conglomerates, interbedded sandstones and subordinate siltstones (Fig. 1c).

The Musayr Formation in the study area generally overlies the Precambrian rocks with a major unconformity, but at some localities it unconformably overlies the Sharik Formation as well (Fig. 1c). Motti et al. (1982) provisionally assigned this formation (lowest part of the Raghama Group) to early Miocene. The Musayr Formation of discontinuous outcrops in the area is divided into three units. They are conglomerate and sandstone (that become finer upward), beds of calcareous sandstone and reworked limestone. The Nutaysh Formation rests conformably on the Musayr Formation and is characterized by coarse detrital- to fine-grained shallow marine sedimentary rocks (Fig. 1c). The rocks of Nutaysh Formation are categorized by an alternate sequence of yellow marl, sandstone and red limestone that changes laterally to conglomerate and sandstone.

Methodologies Used

Remote Sensing Methods

Remote sensing techniques are used to generate an enhanced and interpretable image of the study area. One of the main advantages of remote sensing method is its synoptic view, which can be used to delineate regional and integrated images of various land features. The availability of multi-spectral & high resolution data together with advanced digital image processing techniques has further enhanced the potential of remote sensing in delineating lithological contacts and geological structure in great details and better accuracy (Drury 1987). The use of satellite data in the shape of Landsat imageries provides a powerful tool for geological mapping. A digital format of these data allows applying image processing for extracting useful information and their eventual use in geological mapping. Different remote sensing techniques, such as band ratio and image classification, have been widely used to discriminate between different materials based on their

spectral properties. The Landsat-7 satellite was first launched in April 1999 as part of NASA's Earth Observing System (EOS) system (Goward et al. 2001). The ETM+ sensor of this satellite has the same seven spectral bands as the Landsat-5 Thematic Mapper (TM), but has an added panchromatic band 8 of 15 m resolution together with a higher resolution 60 m thermal band. The Landsat satellites orbit at an altitude of 705 km and have a temporal resolution of 16-day. These satellites were also designed to collect data over a 185-km swath. The Landsat 7 ETM+ has been described as a passive system because it relies on sunlight reflection from the Earth to image the surface. The Landsat-7 data used in this study are taken from the FAST-L7A, which are radiometrically and geometrically corrected. These data sets were acquired on January 6, 2003 from 6 channels. The infrared thermal channel ETM+ 6 is, however, not used for this study. Processing of Landsat 7 ETM+ data was performed using ENVI 5.1 (Environment for Visualizing Images) software. Individual description of each method is given in the following sections.

Red–Green–Blue (RGB) Color Combination Band Images

The RGB color combination images from Landsat 7 ETM+ are primarily selected based on reflectance spectra of dominant rock types in the study area. The 7–4–2 Landsat ETM+ images are used to map the area geologically, i. e., to record different morphological features and to get a display of different rock units in different colors because the Visible-Near Infrared (VNIR) and the Shortwave-Infrared (SWIR) portions of electromagnetic spectrum bands are used (Abdelsalam et al. 2000). The SWIR bands are effective in lithological mapping because many sedimentary rocks have distinctive spectral signatures in this type of electromagnetic spectrum (Evans 1988).

Principal Component Analysis (PCA)

A PCA method is used to produce uncorrelated output bands, to segregate noise components and to reduce dimensionality of the data sets (Richards 1999). Because multispectral data bands are often highly correlated, the principal components (PC) transformation is carried out to produce uncorrelated output bands. This procedure is applied to a new set of orthogonal axes, which have their origin at the mean data and are rotated to maximize the data variance The ENVI 5.1 software has a capability to complete the forward and inverse PC rotations.

Band-Ratio Images

The band ratio images are used to suppress variations in the topography, reflectance, and brightness (related to grain size). These images can also emphasize differences in the shape of spectral reflectance curves (Sultan et al. 1987). In addition, the band ratio images generated from remote sensing data can differentiate between different rock types in a better way compared to those from the RGB color combination (Abdelsalam et al. 2000). The band-ratio images are produced by dividing digital number (DN) values of pixels in bands with high total reflectance by the DN values of corresponding pixels in a band with low total reflectance. Band selection for different ratio images is made here by taking in to account spectral signatures of the dominant lithological units of the area (Abdelsalam et al. 2000). Following the method of Crippen (1989), different ratios, including the short wavelength bands (i.e., 3/1, 4/1 or 4/2), the long wavelength bands (5/ 7) and a combination of these bands (e.g., 5/4 or 5/3) are used here.

The Rf/ φ Method

The R_f/ φ technique is, in fact, based on calculating the theoretical distribution of final ellipticities and orientations after imposing different strains on the objects of known initial ellipticity and orientation. The final ellipticity ($R_{f)}$ and the final orientation (φ) of a deformed object depend on the initial ellipticity (R_i) and the initial orientation (θ) of the undeformed object as well as on the ellipticity ($R_{s)}$ of the imposed strain. In order to evaluate the initial feldspar fabric, the strained features of feldspar grains are un-deformed using the procedure (THETA) of Peach and Lisle (1979). This procedure superimposes the long axis of coaxial strain at right angle to preferred orientation of R_f/ϕ distribution. The magnitude of this superimposed strain is incremented, and the randomness of the resultant un-deformed orientation is calculated after each step. If no initial fabric is present, a reciprocal finite strain can be determined and used to bring the most uniform particle distribution.

The Fry Method

This method, proposed by Fry (1979), is useful to determine the strain ellipsoids from large number of points. In essence, it involves plotting the length and orientation of a large number of center-to-center lines relative to single reference point. The author proposed an object to object separation technique, where the relative positions of adjacent grains are directly plotted by sequentially putting the origin of an overlay on each centre and recording the positions of adjacent centers as points. In many aggregates, these points define an elliptical void and parallel ring of high point-density around the origin of an overlay. These ellipses equal the finite-strain ellipses for homogeneously deformed populations of originally uniform centers. The advantage of Fry method is a graphical solution that it provides from centre-to-centre, which is rapid and accurate. This method is thus considered as an excellent practical technique for finding a best-fitted solution to strain ellipsoids.

Results

Strain Measurements

To quantify the finite strains in meta-granite and metavolcano-sedimentary rocks of Tayyib al Ism area, grains of feldspar, quartz and mafic rocks (such as hornblende, biotite and chlorite) are analyzed by Rf/ϕ and Fry techniques (Fry 1979; Ramsay and Huber 1983). The two-dimensional strain measurements were performed on XY, XZ and YZ sections (X≥ Y≥Z, finite strain axes) to estimate 3D strain geometry. The finite strains determined with normalized Fry technique are primarily used to check the R_f/ϕ estimates. The Fry strains are thought to represent the matrix strain, whereas the R_f/ϕ strains describe the fabric ellipsoid or clasts strain (Ramsay and Huber 1983; Kassem and Abdel Raheim 2010; Kassem 2011; Kassem et al. 2012; Kassem 2012; Al-Saleh and Kassem 2012; Kassem et al. 2013). For the R_f/ϕ analysis on feldspars, hornblende, biotite and chlorite, the long and short axes of up to 40 grains per section are measured and a mean aspect ratio for each section is calculated. Tectonic strains are determined from the chi-squared minima of R_f/ϕ analyses (Peach and Lisle 1979). In the case of Fry analysis, the central points of more than 100 feldspar grains per section are used to estimate strain, which are then used to calculate a finite strain ellipsoid according to the modified least-square technique of Owens (1984).

For these procedures, 20 metavolcanic-sedimentary and meta-granite samples were collected from Tayyib al Ism area (Fig. 1c). Among the collected samples, 9 are metavolcanic from Hegaf Formation, 4 are diorite-gabbro from Swawing Complex, 2 are metagranite from Ifal suite and 5 are from Zuhd alkali granite. The R_f/ϕ method is applied to quartz and feldspar porphyroclasts as well as to mafic grains to find a record of strain in the metavolcano-sedimentary rocks. For the R_f/φ analyses, thin sections were prepared along three mutually perpendicular planes (sub-parallel to XY, YZ and XZ principal planes). Scanned images of the sections, with feldspar and mafic grains marked, are captured and digitized. A least square best-fitting ellipsoid was calculated for each marker as well as its relative position and orientation. In addition to finite strain calculations through computer, the RJH Strain Calculator 3.1 program is used to obtain and plot the strain data.

Stereographic projections of the finite strain analysis for metavolcano-sedimentary rocks of the study area are shown in Fig. 3. These projections indicate that long axes of the finite strain ellipsoid (Maximum Extension Direction along X-axes) in the studied rocks are trending towards ENE-WSW and plunging gently towards ENE (Fig. 2). The intermediate Y axes, on the other hand, trend towards NW/SE with shallow plunging (Fig. 2). As shown in Fig. 2, the maximum shortening direction (Z-axes) indicate steep plunging with a significant clustering. It can thus be concluded that the sub-vertical mean finite shortening axes are due to sub-horizontal foliation in the rocks.

The metavolcanic-sedimentary and metagranite rocks of the study area contain different phases of feldspar, quartz, hornblende and mica. The deformation features in the plagioclase and K-feldspar is rather similar, but that of mica minerals is different from felsic grains. Otherwise quartz is the strongest phase. The results indicate no significant difference in deformation features (induced by peak metamorphic conditions through finite strain) between the quartz-mica matrix, the feldspar porphyroclasts and the amphibole grains. The obtained results further reveal that the finite strain in the studied rocks is at the same order of magnitude, i. e., the main-phase of foliation is similar both in the metavolcanic-sedimentary and metagranite rocks.

The plot of strain data shows the relative shapes of the ellipsoids, i.e., prolate and oblate. Information on volume strain is required to infer the strain type, such as constricted or flattened. The strain ellipsoids identified here have oblate strain symmetry. In case of the R_f/ϕ method, the axial ratios in XZ sections range from 1.70 to 4.80 and in S_X section they are from 1.24 to 1.93. For the Fry method, the axial ratios in XZ sections are in a range between1.50 and 4.50 and in S_X section they are from 1.09 to 1.95. The stretches in Z direction (S_Z) range from 0.41 to 0.73, indicating a vertical shortening of 27 to 59 % for R_f/ϕ method. The ratios in S_Y direction range from 1.01 to 1.26 for the R_f/ϕ method and 1.01 to 1.31 for the Fry method, showing an extensional behavior in this direction. The strain data generally show the same order of deformation in all rock types, which is consistent with the qualitative results obtained from field-based studies and the thin section observations.

The strain symmetry expressed by K value is in a range between 0.10 and 0.94, indicating low to strong oblate ellipsoids for the studied rocks. The strain magnitudes in metavolcanic-sedimentary and metagranite rocks of Tayyib al Ism area are in a range between 0.130 and 1.145, indicating a low to moderate heterogeneous deformation. Field-based observations, however, does not show any obvious relationship between the strain magnitude and tectonic contacts in Tayyib al Ism area.

Remote Sensing

A part of study area is selected to examine the utility of Landsat 7 ETM+ data for lithological mapping. The 7–4–2 Landsat ETM+ image represents the RGB color combination image that is used to discuss the utility of multi-spectral optical bands images for geologic mapping. This bands combination is the best among the available combinations for showing geology of the study area.

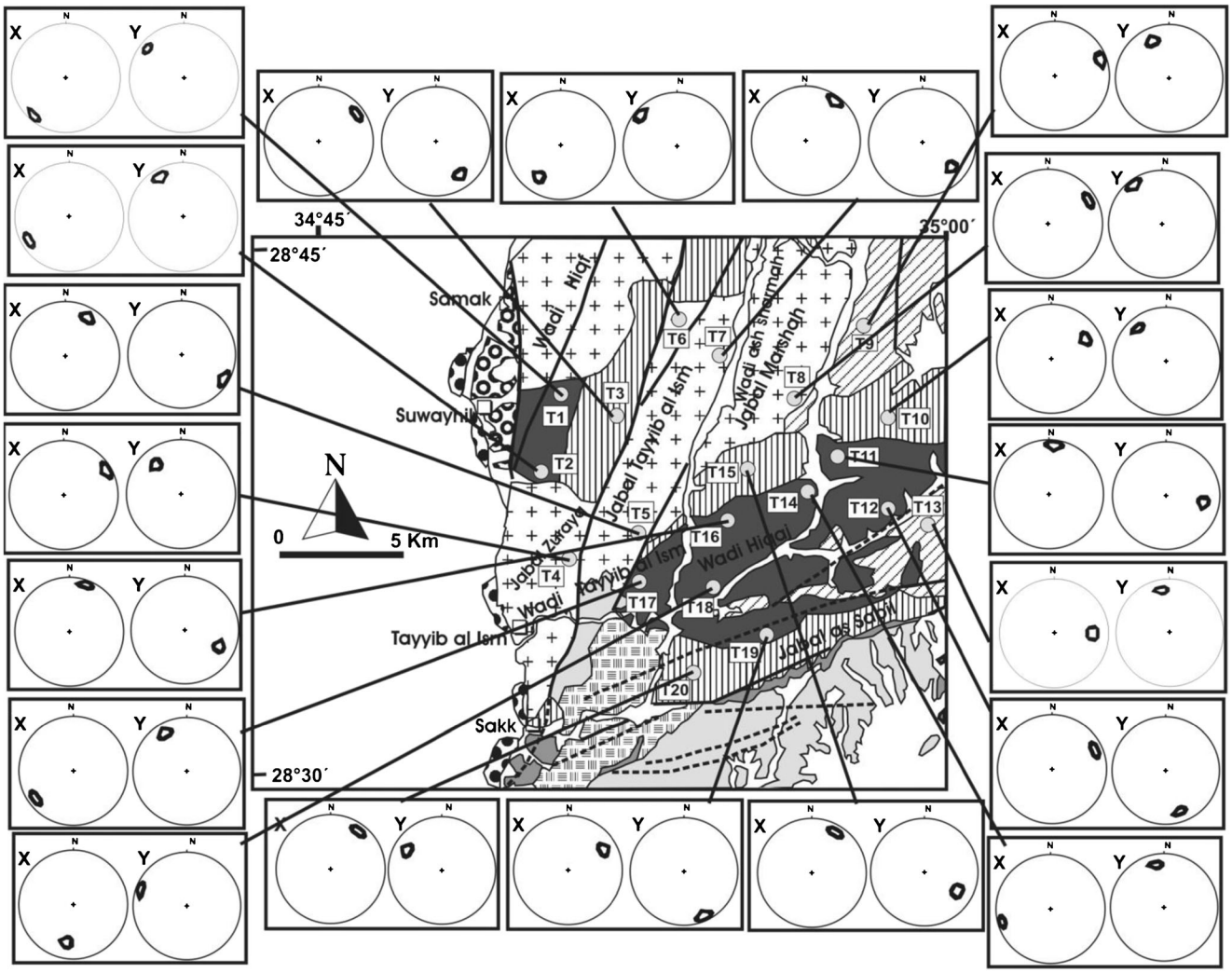

Fig. 2 The lower-hemisphere equal-area projections of maximum extension direction (X) and intermediate direction (Y) are pointed on the geological map of Tayyib al Ism area. The sampled locations are also marked on the map

The PCA bands 3, 2 and 1 in RGB for the study area are shown in Fig. 3a. Almost all rock units covering the study area are discriminated by this false color composite PCA image, where rocks are shown in yellow to orange pixels. The meta-volcanic rocks appear in magenta color, the alkali granites in green color and the monzogranites in red color. Visual interpretations of these images are compared with the published geological map of the study area (Fig. 1c). The images of band

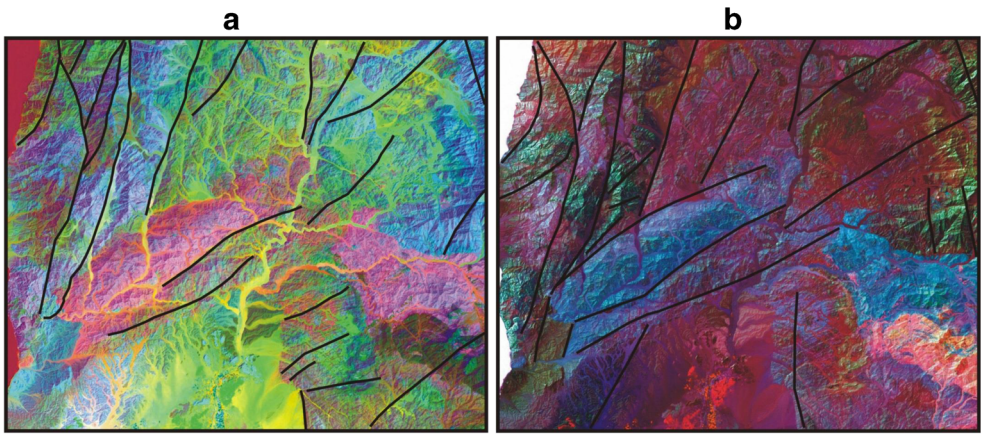

Fig. 3 **a** A color composite of the first three PCA Eigen-channels depicted in green (PCA 1), *blue* (PCA 2) and *red* (PCA 3) for Landsat-7 ETM+. **b** Band ratio image of the study area. Red=7/5, blue=3/1, and green=5/3. The *lines* in this figure represent faults in Tayyib al Ism area

ratios 3/1, 5/3, and 7/5 are identified as the best for showing the lineament features in the study area (Fig. 3b). These ratios indicate that most of the major faults are distributed in the northwestern and southwestern parts of the study area. In addition, some minor faults are distributed along the Gulf of Aqaba coast as well.

Structural and Tectonic History

The study area is located in the Midyan region of northwestern Saudi Arabia. This area, which is bounded by the Red Sea on one side and the Gulf of Aqaba on other side, is characterized by major faults. The major faults in the Midyan region include: (1) the northwest trending Najd Fault system (2) the north-northwest (NNW) trending Red Sea faults system and (3) the NNE trending Gulf of Aqaba system. The area under investigation is dominantly dissected by the Gulf of Aqaba system. Many easterly directed faults can also be observed in the area. Most of the faults in the region are probably late Proterozoic in age, which get reactivation during the Tertiary.

The Midyan region is located just north of the late-Proterozoic Najd wrench-fault system, along which a cumulative left-lateral movement of about 240 km has occurred (Moore 1979). The most northerly located major structure related to Najd fault system is the Muwaylih fault zone (Ramsay et al. 1985) in Al Muwaylih area. A continuation of this structure is probably concealed beneath the sands and gravels of the Ash Shaykh Humayd Peninsula in the southwestern corner of the Midyan region. Some fault zones in the area are considered as the structural boundaries between the provinces of different ages.

Gabbroic dikes (probably Tertiary in age) are present along the traces of faults at several places. In addition, the mafic dikes also extend away from the lineaments into the country rocks for as much as several kilometers. These dikes are Tertiary or older in age. Other researchers (Motti et al. 1982) have reported that faults having a Red Sea trend were active as far back as the Paleozoic. These faults might be even older because rocks of the Minaweh Formation in the north-northwest-trending "Aynunah and Sharmah troughs (grabens) remained un-affected by erosion since the late Proterozoic. In the southwestern part of the region, an intersection of the Red Sea and the Gulf of Aqaba fault systems has produced a wedge-shaped depression in the shape of Ifal basin.

The faults associated with the Gulf of Aqaba system are most obvious within a few kilometers of the coast. Up to hundred of kilometers movements, both in normal and sinistral sense, have been observed along the individual faults. A total movement along the Gulf of Aqaba-Dead Sea rift is estimated to be about 105 km. Geological observations of the gulf area suggest the presence of three elongated-enechelon basins filled with 2 to 3 km thick clastic sediments (turbidites and pelagic deposits).

Discussions

According to Makris and Henke (1992) observations, the Arabian Plate is moving away from Africa towards north, causing the Red Sea opening and an eventual thinning of the continental crust under the Saudi Red Sea coast. During the middle to late Miocene, a left-lateral fault movement commenced in the Gulf of Aqaba and along the Dead Sea rift. The northeast trending en-echelon anticlines in the study area are consistent with the major left-lateral strike-slip fault system in the Gulf of Aqaba (Hughes et al. 1999). The topography and structure of the area reflect that margin of the Saudi Red Sea coast is tectonically segmented and has undergone different uplift events (Roobol and Stewart 2009). Other researchers divided the Red Sea succession into discrete regional depositional events. Several tectonic episodes have been suggested for the Red Sea region. The tectono-geological events experienced by Midyan region are summarized as pre-rift and syn-rift in origin.

The present results reveal that the Hegaf belt of volcanic and sedimentary rocks are associated with the vertical faults and small graben structures, indicating a change from compressional to tensional tectonics in the late Proterozoic (Clark 1986). The present field observations and strain data support a notion that metagranitic and metavolcano-sedimentary rocks of the area were deformed by younger granitic intrusions along the faults. These rocks are foliated along the ENE-WSW directions in Tayyib al Ism area (Fig. 2). In addition, the granite intrusions were rounded in a roughly north–south direction. In these rocks, the deformation induced stretched lineations are trending in E to ENE direction and the associated kinematic indicators record ENE tectonic transport (Fig. 2). The present study also supports that the supra-structural nappes in Midyan region of northwestern Saudi Arabia were first intruded by diorites, gabbros and metagranites, and then by alkali granite.

A fault drag along the Gulf of Aqaba fault zone can be observed by conspicuous changes in the direction of dike swarms. A similar pattern is observed in the east-striking faults as well, which is currently making a curvilinear trend towards the coast. This type of behavior indicates a fairly recent movement along the Gulf of Aqaba fault zone, where the north-northwest striking faults are experiencing some sort of activities, as evident from the occurrence of earthquakes in Haql and Dead Sea valley areas during 1983. Al-Tayyar et al. (1982) have reported that the Proterozoic faults in the area were reactivated during the Red Sea opening. They are apparently not related to the transform structures of the axial zone in the Red Sea trough, which were originally directed towards

east-northeast. Both the left-lateral and right-lateral movements have been observed along these faults (Al-Tayyar et al. 1982). Other faults of variable orientation are also present in the region, which could probably be Proterozoic in age.

A significant relationship between the strain magnitude and tectonic contacts of the study area may have two explanations: (1) the nappe contacts were formed during granitic intrusions under the brittle to semi-ductile deformation conditions much before the area was affected by high-pressure metamorphism. As a result of this metamorphism, a ductile strain heterogeneously superimposed the already assembled nappe structure. (2) The nappe contacts were formed after a cease in high-pressure metamorphism, i.e., a ductile strain in the area accumulated before the nappes were formed.

It is suggested, that contacts between the granites and the surrounding rocks in the Tayyib al Ism area were formed during their intrusions under the brittle to semi-ductile conditions before the area was affected by metamorphism. Apparently, the finite strain accumulated in the area during metamorphism indicates that the nappe contacts were formed before the accumulation of finite strain. Furthermore, the main-phase foliation is not different for all types of rocks, which also suggest similar deformation behavior in all types of rocks. The data shows significant relationship between the strain magnitude and the tectonic contacts in the Tayyib al Ism area. Also, the strain type as expressed by the K value does not show a distinct pattern in the Tayyib al Ism area. Deformation was accompanied by vertical shortening and this explains flattening strain type in large parts of the Tayyib al Ism area. Furthermore, the orientation of the metagranite and metavolcano-sedimentary rocks was retained throughout the main deformation events in the region.

Conclusion

1. The results obtained by present study suggest that metagranites and metavolcano-sedimentary successions of Tayyib al Ism area are affected by the same deformation events. Hence, the finite strain in the deformed granites has the same magnitude as that of the metavolcano-sedimentary rocks.
2. The here presented data further indicate that the studied rocks are characterized by subvertical shortened axes, which are associated to sub-horizontal foliations.
3. Analyses of the Landsat 7 ETM+ imageries (including the Principal Component Analysis and Band Ratio methods) proved successful in mapping geological lineaments and features in the study area.
4. The obtained data also indicate the presence of flattening strain symmetries in Tayyib al Ism area.
5. An increase in the magnitude of Nadai strain indicates a relationship between the strain magnitude and tectonic contacts in Tayyib al Ism area, which were formed during granitic intrusions along the fault zones under brittle to semi-ductile deformation.
6. The finite strain accumulated in the studied rocks by high-pressure metamorphism reveals the formation of nappe contacts intrusion of granitic plutons.

Acknowledgments The authors would like to extend their sincere, appreciation to the Deanship of Scientific Research at King Saud University for funding this research group NO. RG1435-008. Thanks are also due to the reviewers for their critical and helpful comments.

References

Abdelsalam, M., Stern, R. J., & Berhane, W. G. (2000). Mapping gossans in arid environments with Landsat TM and SIR-C images: the Beddaho alteration zone in northern Eritrea. *Journal of African Earth Sciences, 30*, 903–916.

Al-Saleh, A. M., & Kassem, O. M. K. (2012). Microstructural, strain analysis and $^{40}Ar/^{39}Ar$ evidence for the origin of the Mizil Gneiss Dome, Eastern Arabian Shield, Saudi Arabia. *Journal of African Earth Sciences, 70*, 24–35.

Al-Tayyar, J.A. Al-Otaibi, R.H., & Rowainy, M.N. (1982). Reconnaissance geology of the Jabal al Lawz quadrangle, sheet 28/36 A. Kingdom of Saudi Arabia: Saudi Arabian Deputy Ministry for Mineral Resources Open File Report DGMR-OF-02-15, 23p.

Clark, M.D. (1986). Explanatory notes to the geologic map of the Al Bad' quadrangle, sheet 28A, Kingdom of Saudi Arabia. Saudi Arabian Deputy Ministry for Mineral Resources Geoscience Map Series GM- 81A, C, scale 1:250,000, with text, 46 p.

Crippen, R. E. (1989). A simple spatial filtering routine for the cosmetic removal of scan-line noise from Landsat TM P-tape imagery. *Photogrammetric Engineering and Remote Sensing*, 55(3), 327–331.

Davies, F.B., & Grainger, D.J. (1985). Geologic map of the Al Muwaylih quadrangle, sheet 27 A. Kingdom of Saudi Arabia: Saudi Arabian Deputy Ministry for Mineral Resources Geoscience Map GM-82A. C. scale 1:250,000, with text. 32p.

Drury, S. A. (1987). *Image interpretation in geology*. London: Allen & Unwin.

Evans, D. (1988). Multi-sensor classification of sedimentary rocks. *Remote Sensing of Environment, 25*, 129–144.

Fry, N. (1979). Random point distributions and strain measurement in rocks. *Tectonophysics, 60*, 89–105.

Gardner, W. C., Khan, M. A., & Al-Hinai, K. G. (1996). Interpretation of Midyan and Sinai Geology from a Landsat TM image. *Arabian Journal for Science and Engineering, 21*(4A), 571–586.

Goward, S. N., Masek, J. G., Williams, D. L., Irons, J. R., & Thompson, R. J. (2001). The Landsat 7 mission. *Remote Sensing of Environment, 78*, 3–12.

Hughes, G. W., Perincek, D., Grainger, D. J., Abu-Bshait, A., & Jarad, A. M. (1999). Lithostratigraphy and depositional history of part of the Midyan region. Northwest Saudi Arabia. *GeoArabia, 4*(4), 503–542.

Johnson, P. R. (1998). The structural geology of the Samran-Shayban area, Kingdom of Saudi Arabia: Saudi Arabian Deputy Ministry for Mineral Resources Technical Report USGS-TR-98-02, 45 p.

Johnson, P. R., & Kattan, F. (2001). Oblique sinistral transpression in the Arabian shield: the timing and kinematics of a Neoproterozoic suture zone. *Precambrian Research, 107*, 117–138.

Johnson, P. R., Abdelsalam, M. G., & Stern, R. J. (2003). The Bi'r Umq-Nakasib suture zone in the Arabian-Nubian Shield: a key to understanding crustal growth in the East African Orogen. *Gondwana Research, 6*, 523–530.

Kassem, O. M. K. (2011). Determining heterogeneous deformation for granitic rocks in the Northern thrust in Wadi Mubark belt, Eastern Desert, Egypt. *Geotectonics Journal, 45*(3), 244–254.

Kassem, O. M. K. (2012). Kinematic *vorticity analysis Technique for Porphyroclasts in the Metamorphic Rocks, an example from the* Northern thrust in Wadi Mubarak belt, Eastern Desert, Egypt. *Arabian Journal of Geosciences, 5*(1), 159–167.

Kassem, O. M. K., & Abdel Raheim, S. (2010). Finite strain analysis for the Metavolcanic-sedimentary rocks in the Gabel El- Mayet region, Central Eastern Desert, Egypt. *Journal of African Earth Sciences, 58*, 321–330.

Kassem, O. M. K., Abd El Rahim, S. H., & El Nashar, E. R. (2012). Strain analysis and Microstructural evolution characteristic of Neoproterozoic rocks associations of Wadi El Falek, Centre Eastern Desert, Egypt. *Geotectonics, 46*(5), 379–388.

Kassem, O. M. K., Al Bassam, A. M., & Zaidi, F. K. (2013). Structural and mechanical controls on intrusion related to Mahd ad Dahab area, Arabian Shield, Saudi Arabian. *Journal on Geological Sciences, 1*(1), 63–72.

Makris, J., & Henke, C. H. (1992). Full apart evolution of the Red Sea. *Journal of Petroleum Geology, 15*(2), 127–134.

Moore, J. M. (1979). Tectonics of the Najd transcurrent fault system. *Saudi Arabia: Journal of the Geological Society of London, 136*, 441–454.

Motti, E., Teixido, L., Vazques-Lopez, R., & Vial, A. (1982). Maqna Massif area: Geology and Mineralization. Saudi Arabian Deputy Ministry for Mineral Resources Open File Report BRGM-OF-02-16, 44p.

Nehlig, P., Genna, A., & Asfirane, F. (2002). A review of the Pan-African evolution of the Arabian shield. *GeoArabia, 7*, 103–124.

Owens, W. H. (1984). The calculation of a best-fit ellipsoid from elliptical sections on arbitrarily oriented planes. *Journal of Structural Geology, 6*, 571–578.

Peach, C. J., & Lisle, R. J. (1979). A fortran IV program for the analysis of tectonic strain using deformed elliptical markers. *Computers and Geosciences, 5*, 325–334.

Ramsay, J. G., & Huber, M. I. (1983). *The techniques of modern structural geology* (Strain analysis, Vol. 1). New York: Academic.

Ramsay, C.R. Drysdall, A.R., & Clark, M.D. (1985). Felsic plutonic rocks of the Midyan region, Kingdom of Saudi Arabia. Pt. 1: Distribution, classification and resources potential. In A. R. Drysdall, C. R. Ramsay, & D. B. Stoeser (eds.), Felsic plutonic rocks and associated mineralization of the Kingdom of Saudi Arabia: Saudi Arabian Deputy Ministry for Mineral Resources Bulletin 29, p. 63–77.

Richards, J. A. (1999). *Remote sensing digital image analysis: An introduction* (p. 240). Berlin: Springer.

Roobol, M.J., & Stewart, I.C.F. (2009). Cenozoic faults and recent seismicity in northwest Saudi Arabia and the Gulf of Aqaba region. Technical report SGS-TR-2008-7, 35 p.

Stoeser, D. B., & Camp, V. E. (1985). Pan-African microplate accretion of the Arabian Shield. *Geological Society of America Bulletin, 96*, 817–826.

Sultan, M., Arvidson, R. E., Sturchio, N. C., & Guinnes, E. A. (1987). Lithologic mapping in arid regions with Landsat TM data: Meatiq dome, Egypt. *Geological Society of America Bulletin, 99*, 748–762.